frontiers | Frontiers in Energy Research

TYPE Methods
PUBLISHED 26 September 2022
DOI 10.3389/fenrg.2022.967856

Predicting the reaction efficiency of ginkgo biloba residues pyrolysis by using artificial intelligent algorithms under the background of Carbon Neutrality

Li Liu[1†], Zhenwei Yu[2†], Zheqi Chen[1], Kai Wang[3], Qian Xiao[1] and Jingjing Chen[4*]

[1]School of Economics and Social Welfare, Zhejiang Shuren University, Hangzhou, China, [2]College of Mechanical and Electronic Engineering, Shandong Agricultural University, Taian, China, [3]College of Automation and Machinery, Weifang University, Weifang, China, [4]Zhejiang University City College, Hangzhou, China

OPEN ACCESS

EDITED BY
Yang Du,
James Cook University, Australia

REVIEWED BY
Lu Xu,
Jiangsu Normal University, China
Guobao Xu,
Northwest Institute of Eco-Environment and Resources (CAS), China
Xinlei Yi,
Royal Institute of Technology, Sweden

*CORRESPONDENCE
Jingjing Chen,
joyjchan@gmail.com

†These authors have contributed equally to this work and share first authorship

SPECIALTY SECTION
This article was submitted to Process and Energy Systems Engineering, a section of the journal Frontiers in Energy Research

RECEIVED 23 June 2022
ACCEPTED 29 August 2022
PUBLISHED 26 September 2022

CITATION
Liu L, Yu Z, Chen Z, Wang K, Xiao Q and Chen J (2022), Predicting the reaction efficiency of ginkgo biloba residues pyrolysis by using artificial intelligent algorithms under the background of Carbon Neutrality.
Front. Energy Res. 10:967856.
doi: 10.3389/fenrg.2022.967856

Since the beginning of 2016, China's annual emissions of herbal residues (HR) have exceeded 30 million tons. As a kind of solid waste, HR still contains a large amount of organic matter, which requires further industrial extraction procedure. Most of the existing studies are concerned with the feasibility of utilizing traditional Chinese medicine residues, meanwhile there are very few studies regarding the kinetics of pyrolysis in the process of resource utilization of traditional Chinese medicine residues. In this study, we comprehensively studied the kinetics characteristics of raw materials with various heating rates (10, 20, 30, and 40°C/min) using a synchronous thermogravimetric analysis, and we adopted Coats-Redfern model to study the thermal kinetics and thermal analysis of GBR. A novel method combining Genetic algorithm and Adaboost algorithm (GA-Adaboost) is proposed to predict the thermogravimetric curve of the raw plant material with respect to the heating rate and temperature. The experimental result shows that the activation energy of the raw material was determined by the Kissinger-Akahira-Sunose (KAS) ($E = 148.71 kJ/mol$), and the correlation coefficient was greater than 0.99. The optimal reaction mechanism determined by the Coats - Redfern method was random nucleation and subsequent growth. The GA-Adaboost model achieved good performance (with a fitting degree of 99.88% on training data, 99.80% on verification data, and MSE of3.4173) while predicting the pyrolysis process of ginkgo biloba residue. This study will provide theoretical basis and technical support for the efficient resource utilization of pharmaceutical residues and reduce environmental pressure.

KEYWORDS

genetic algorithm, adaboost algorithm, herb residue, pyrolysis kinetics, predictive model

1 Introduction

The rapid development of global industrialization has led to extreme dependence on the demand for petrochemical energy, such as coal and oil (Chen et al., 2017a; Bai et al., 2018; Zhang et al., 2018). With the massive consumption of petrochemical energy and the increase of environmental pollution, developing sustainable energy sources is an extremely urgent need. Biomass resources are full of carbon matter, and are with large reserves and in a wide distribution (De Sales et al., 2017). Moreover, the utilization process of biomass resources has the advantages such as low pollution, renewable, and thus is considered a potential alternative to petrochemical energy. Biomass energy refers to the energy present in biomass, such as wood, straw, vegetable oil and various industrial wastes. However, currently, biomass resources have not been fully utilized (Pelaez-Samaniego et al., 2013). Most of the biomass is used directly for combustion, which is inefficient and pollutes the environment. Converting biomass into liquid, solid or gaseous fuel can not only reduce dependence on petrochemical energy but also alleviate the environmental pressure caused by greenhouse gas emissions, which have profound significance for ensuring the energy supply, improving the environment and sustainable development (Chen et al., 2017b).

Since the beginning of 2016, China's annual emissions of herbal residues (HR) have exceeded 30 million tons (Yu et al., 2019). As a solid waste, HR still contains a large amount of organic matter within the industrial extraction procedure. Wang et al. used catalytic pyrolysis to process HR, and successfully obtained biological oil, which provided a technical opportunity for the efficient utilization of HR (Shen et al., 2022). The experimental result shows that the optimum pyrolysis temperature of this raw material was449.9℃, and the highest yield rate of biological oil was 39%. Guo et al. studied the gasification characteristics of HR. In a pilot-scale circulating fluidized bed, the air was used as a kind of gasifying agent, and the calorific value of the product gas exceeded $4.0MJ/N\cdot m^3$(Guo et al., 2013). Most of these studies focused on the feasibility of resource utilization of traditional Chinese medicine (TCM) residues, but the kinetics of pyrolysis and related reaction mechanisms of TCM in the resource utilization process are rarely mentioned.

Adaboost algorithm and genetic algorithm (GA), are usually used to address nonlinear problems. Adaboost algorithm was proposed by Freund and Schapire (Freund, 1995). Its main idea is to use a large number of trained weak classifiers to form a strong classifier with better classification performance in some way (Zhang et al., 2021; Lu et al., 2022). GA can directly optimize structural objects, and is a kind of efficient global search methods (Wang et al., 2020; Zhou et al., 2021a; Yan, 2021). In this study, in order to improve the efficiency of ginkgo biloba residue (GBR) pyrolysis, the kinetics characteristics of raw materials with various heating rates were comprehensively studied using a synchronous thermogravimetric analysis. A novel method combining GA and Adaboost (GA-Adaboost) is proposed to predict the thermogravimetric curve of the material with respect to the heating rate and temperature. The contribution in this work is summarized as:

1) Proposed an novel method for predicting the thermogravimetric curve of the material with respect to the heating rate and temperature.
2) A comprehensive survey on the kinetics characteristics of raw materials with various heating rates were conducted.
3) An experiment based on materials from pharmaceutical manufacturer was carried out, and the experimental result shows the proposed method could significantly improve the efficiency of the reaction mechanism.

2 Related literatures

Genetic algorithm (Holland, 1992) is an adaptive global optimization algorithm, which is based on a natural population genetic evolution mechanism. Genetic algorithm is usually used for multi-objective optimization, and has been widely adopted in many sectors. E.g., Guerrero et al. (Guerrero et al., 2018) proposed Non-Dominated Sorting Genetic Algorithm II (NSGA-II) to optimize the allocation of containers in cloud architectures. Qiu al (Qiu et al., 2015) proposed task scheduler for a chip multiprocessor to efficiently allocate memory usage and improve system performance. Gai et al. (Gai et al., 2017) proposed Dynamic Data Allocation Advance (2DA) algorithm for data allocation in multimedia applications. Mayer et al. (Mayer et al., 2020) used genetic algorithm to solve multi-objective scaling problems for building-scale microgrids with regards to the economic and environmental factors. Besides, Li (Li et al., 2021) et al. proposed a convenient and fast framework for multi-objective optimization of proton exchange membrane fuel cell (PEMFC). Starke et al. (Starke et al., 2018) introduced genetic algorithm to the context of solar power plant sizing, which allows the evaluation of the plant performance as well as the optimal configuration from the obtained data. Panapakidis et al. (Panapakidis and Dagoumas, 2017) introduced the combination of genetic algorithm and neural network to forecast the natural gas demand.

The combination of genetic algorithms and other technologies can solve practical problems efficiently and accurately. Zhou et al. (Zhou et al., 2021b) combined genetic algorithm with hydrodynamic simulations to optimize diesel/gasoline dual-mode dual fuel combustion in compression-ignition engines, and it is used to optimize parameters that have a critical impact on engine performance and emissions. Singh et al. (Singh et al., 2020) proposed the use of genetic algorithm combined with structural equation modeling to

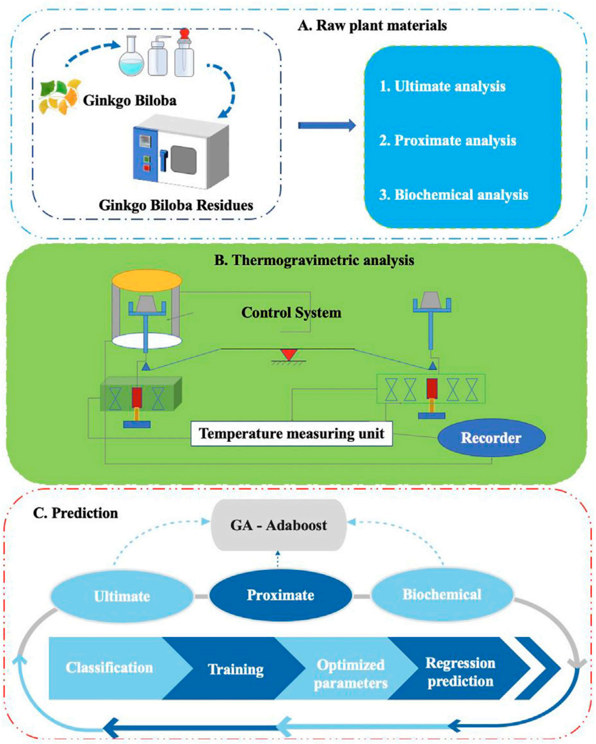

FIGURE 1
The workflow of the method: **(A)**. Processing the raw plant materials; **(B)**. Thermogravimetric analysis; **(C)**. GA-Adaboost based prediction.

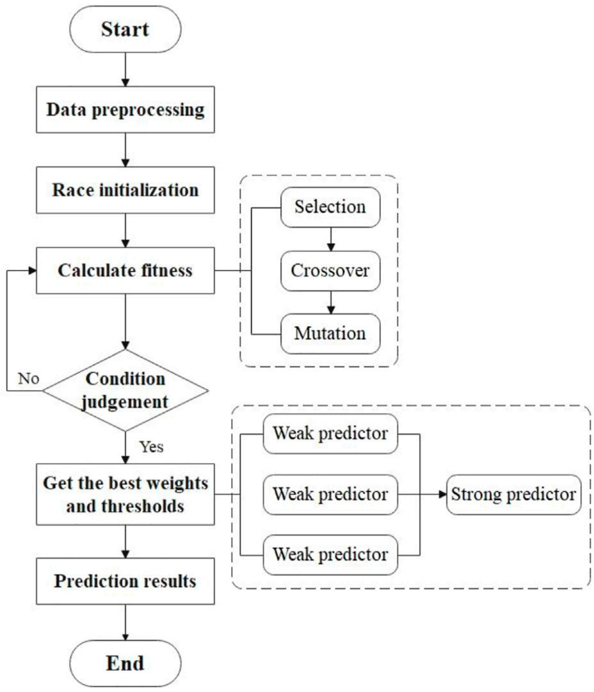

FIGURE 2
The main workflow of applying GA to Adaboost parameter optimization.

predict commercial aviation fuel combustion and to optimize it. Paykani et al. (Paykani et al., 2019) used a non-dominated ranking genetic algorithm combined with an ideal solution similarity ranking priority technique to solve the problem of inability of the GRI-Mech 3.0 mechanism to accurately predict the combustion characteristics of methane fuel mixtures and to determine the optimal methane fuel mixture ratio. Nazoktabar et al. (Zhou et al., 2022a) proposed a method combining genetic algorithm with a thermal dynamics model to optimize the performance and predict the emissions of homogeneous compression-ignition engines.

The Adaboost algorithm (Nazoktabar et al., 2018) focuses on training a dataset to obtain multiple classification results and integrating them to distinguish samples by weighting the misclassified samples. Adaboost has been applied in many contexts. E.g., Adaboost is used with sensors in mobile devices (Freund and Schapire, 1996) for identifying daily activities and environments. Esmaeili et al. (Zhou et al., 2022b) applied Adaboost to detect indoor/outdoor environments by extracting features from different actions of users and subsequently using Adaboost integrated with random forest to classify environment types with an accuracy higher than 99%, Caiet al (Ferreira et al., 2020) proposed an improved Adaboost algorithm (named Twi-Adaboost) for improving indoor localization accuracy. Adaboost can also be applied to detect false comments (EsmaeiliKelishomi et al., 2019), which can be analyzed based on text features, such as Fitzpatrick et al. (Yan et al., 2022a) using verbal and non-verbal as cues for analysis. Adaboost can also be applied to medical contexts, e. g., Huang et al. (Barbado et al., 2019) used Adaboost in combination with machine learning to reduce the computational complexity of critical care data. Wang et al. (Zhou et al., 2021c) proposed an enhanced Adaboost algorithm to tune the weaker classifier parameters. Besides, Adaboost algorithm is also integrated with other technologies in various contexts (Fitzpatrick et al., 2015; Huang et al., 2020; Liang et al., 2021; Wang and Sun, 2021; Yan et al., 2022b).

3 Method

In this study, in order to improve the efficiency of ginkgo biloba residue (GBR) pyrolysis, a novel method combining genetic algorithm and Adaboost algorithm (GA-Adaboost) is proposed to predict the thermogravimetric curve of the material with respect to the heating rate and temperature. The full workflow of the method is illustrated in Figure 1.

3.1 GA-Adaboost model

GA-Adaboostis designed to predict the quality loss of biomass pyrolysis process. Through the Adaboost algorithm, many weak classifiers can be integrated into a strong classifier for prediction/classification, and finally the predicted results will be integrated (Ferreira et al., 2017). Its main advantages are simple and easy-to-use. The upper bound of training error rate gradually decreases with the increase of iterations, and even though the training times are large, there will be no "over learning" phenomenon. The Adaboost algorithm is suitable for classification tasks (Zhan and Yu, 2020). However, it also has some disadvantages. For example, it is easy to be impacted by noise; the computing complexity is high, and it takes a long time to complete the training; for high-dimension data classification, the error is at a high level. In this design, GA is used as weak classifier to form ensemble learning algorithm, and then the optimized parameters are used to train the Adaboost model to achieve high-precision regression and prediction. The proposed method not only makes full use of the advantages of global fast search by genetic algorithm, but also greatly improves the efficiency of optimal parameters selection, and finally improves the prediction accuracy of the model. The main steps applying GA to Adaboost parameter optimization are shown in Figure 2.

mm groups of training data are selected from the dataset, and the weight values of initialization sample data was set as$D_t(i) = 1/m$. According to Eq. 1, the training data is normalized to the distribution in [0, 1].

$$x_i = \frac{x_i - x_{min}}{x_{max} - x_{min}} \tag{1}$$

An initial population was generated randomly, and the population had characteristic strings with definite length (Li et al., 2020). The population was iterated until a suitable population was obtained. In the iteration, the fitness value of each individual in the population was calculated, and the next generation population was generated by replication, crossover and mutation operations.

The individual with the greatest fitness in any generation was designated as the iterative result of the function. This result can be used as the optimal solution, and the optimal weight and threshold can be obtained after decoding.

The GA was used to train the weak predictors and then the trained weak predictors was used to predict the output value $ht(x)$ of the training data, and the absolute value of the prediction error of the weak predictors was calculated. The formula is defined as:

$$e(i) = |h_t(x_i) - y_i| \, (i = 1, 2, \cdots, m) \tag{2}$$

where x_i denotes the input variables of weak predictors; y_i denotes the actual value of comprehensive score. The error sum was calculated according to the formula:

$$\varepsilon_t = \sum D_t(i)(e(i) > \varphi) \tag{3}$$

The calculation to obtain the weight coefficients of weak predictors is formularized as below:

$$w_t = 0.5 \, ln \frac{1 - \varepsilon_t}{\varepsilon_t} \tag{4}$$

According to the weight coefficients, the weight of the next round of training samples would be adjusted. The adjustment formula is defined as:

$$D_{t+1}(i) = \begin{cases} \dfrac{D_t(i)}{B_t} exp \, w_t (e(i) > \varphi) \\ \dfrac{D_t(i)}{B_t} \text{(other)} \end{cases} \tag{5}$$

where $B_t$is a normalization factor, which can summarize the distribution weights of samples, and keep the weight ratio of each component unchanged. It outputs the strong predictors. After training for T times, the T groups weak prediction function was obtained, and the final strong predictors output $F(x)$ was obtained by its weighted combination. Its calculation formula is defined as:

$$F(x) = \sum_{t=1}^{T} w_t f(h_t(x), w_t) \tag{6}$$

3.2 Kinetic theory

TGA is an important tool for studying the thermal decomposition process and analyzing the pyrolysis kinetics of materials. It is designed for measuring the weight loss process of materials with temperature changes, and predicting pyrolysis mechanism in this context. Biomass pyrolysis is a complex process that involves multiple reactions. Generally, a full kinetic analysis of the complex system is not feasible, but some types of average kinetic descriptions could be obtained (Mehmood et al., 2017). In this study, three different kinetic models were used to study the pyrolysis kinetics of the GBR. The TGA data for the GBR was analyzed by applying the equal conversion KAS and Coats-Redfern models. The reaction rate equation is shown in Eqs 7–9.

$$\frac{d\alpha}{dT} = \left(\frac{1}{\beta}\right) k(T) f(\alpha) \tag{7}$$

$$\alpha = \frac{m_0 - m_T}{m_0 - m_\infty} \tag{8}$$

$$\frac{d\alpha}{dT} = \left(\frac{A}{\beta}\right) \exp\left(-\frac{E}{RT}\right) f(\alpha) \tag{9}$$

where a is the conversion value, β (°C/min) is the heating rate, $k(T)$ is the temperature relationship of Arrhenius reaction rate constant, $k(T) = A \exp[-E/(RT)]$, $f(\alpha)$ is the reaction

TABLE 1 Reaction mechanisms, model names with their $f(\alpha)$and $G(\alpha)$.

Model	Code	$G(\alpha)$	$f(\alpha)$
Chemical Reaction, $n = 1$	F1	$-ln(1-\alpha)$	$(1-\alpha)$
Chemical Reaction, $n = 2$	F2	$(1-\alpha)^{-1}-1$	$(1-\alpha)^2$
One-dimensional diffusion, 1D	D1	α^2	$\alpha^{-1}/2$
Two-dimensional diffusion, 2D	D2	$(1-\alpha)ln(1-\alpha)+\alpha$	$[-ln(1-\alpha)]^{-1}$
Three-dimensional diffusion, $n = 2$	D3	$[1-(1-\alpha)^{1/3}]^2$	$3/2(1-\alpha)^{2/3}[1-(1-\alpha)^{1/3}]^{-1}$
Avrami-Erofeev, $n = 2$	A1	$[-ln(1-\alpha)]^2$	$1/2(1-\alpha)[-ln(1-\alpha)]^{-1}$
Avrami-Erofeev, $n = 3$	A2	$[-ln(1-\alpha)]^3$	$1/3(1-\alpha)[-ln(1-\alpha)]^{-1}$
Avrami-Erofeev, $n = 4$	A3	$[-ln(1-\alpha)]^4$	$1/4(1-\alpha)[-ln(1-\alpha)]^{-1}$
Phase boundary reaction of shrinking cylinder, $n = 1/2$	R1	$1-(1-\alpha)^{1/2}$	$2(1-\alpha)^{1/2}$
Phase boundary reaction of shrinking spheres, $n = 1/3$	R2	$1-(1-\alpha)^{1/3}$	$3(1-\alpha)^{2/3}$

mechanism function, m0 (mg) is the initial sample mass, mT (mg) is the sample mass at temperature T, m_∞ (mg) is the remaining mass after reaction, A (min-1) is the frequency factor, E (kJ/mol) is the activation energy, R (J/(KJ/mol)) is the gas constant, T (K) is the absolute temperature.

3.3 KAS model

The KAS model, one of the most widely used equal-transformation methods for calculating pyrolysis kinetics (Collazzo et al., 2017; Mishra and Mohanty, 2018), is formularized as below:

$$\ln\left(\frac{\beta}{T^2}\right) = \ln\left(\frac{AE}{RG(\alpha)}\right) - \frac{E}{RT} \tag{10}$$

Since the same a is selected under different conditions, $G(\alpha)$ is a constant value, and the ln [β/T2]-1/T is plotted to obtain a line, and the activation energy E of the reaction can be obtained through the slope and intercept of the line. The Coats-Redfern model is used to deal with the dynamics of Eq. 11. After shifting the terms and integrating the two sides (Minh Loy et al., 2018), the result is shown as below:

$$\frac{G(\alpha)}{T^2} = \left(\frac{AR}{\beta E}\right)\left[\exp\left(-\frac{E}{RT}\right) - \exp\left(-\frac{E}{RT_0}\right)\right] \tag{11}$$

Where $G(\alpha) = \int_0^\alpha \frac{d\alpha}{f(\alpha)}$, since $\exp(\frac{E}{RT_0}) \approx 0$, taking the natural logarithm on both sides of Eq. 10, Eq. 12 is obtained as below:

$$\ln\left[\frac{G(\alpha)}{T^2}\right] = \ln\frac{AR}{\beta E} - \frac{E}{RT} \tag{12}$$

By plotting $\ln[\frac{G(\alpha)}{T^2}] - \frac{1}{T}$, the exponential factor A and energy E can be respectively calculated by the slope and intercept of the plotted straight line. $G(\alpha)$ can vary according to different development models and reaction mechanisms (Oluoti et al., 2018). Commonly used mechanisms are listed in Table 1.

4 Experiment

4.1 Experimental settings

The raw materials used in this experiment were obtained from SPH Xingling Pharmaceutical Co. The obtained sample consisted of dry ginkgo leaves. The raw material was immersed in a 60% aqueous ethanol solution, and water vapor was continuously introduced. 6 h later, the mixture was filtered and washed to get the GBR. With the operation of cooling, the residue was dried at 80 C for 24 h using an electrothermal oven (101-0BS, Lichen, Shanghai, China). The dried residue was pulverized using a pulverizer (CY-150, Xiji, Zhejiang, China) to a diameter of ≤200 μm.

After the proximate analyses of moisture, ash, volatiles and fixed carbon, the results can be seen in Table 2.

4.2 Thermogravimetric analysis

The pyrolysis characteristics of the GBR were investigated with a thermogravimetric analyzer. The sensitivity of the microbalance was less than ±0.1 μg. The sample (10 ± 0.01 mg) was placed in an aluminum crucible, and the sample weight was continuously measured. In the tube furnace (OTF-1200X, Kejing, Hefei, China), the sample was heated from 800 °C at heating rates of 10 °C/min, 20 °C/min, 30°C/min and 40 C/min under non-isothermal conditions and kept at 105°C for 10 min to ensure complete removal of moisture; then, it was heated from 105 to 800 C. The data obtained from the TGA experiments were used for the kinetic parameter analysis. Nitrogen was used as a type of carrier gas to pyrolyze the sample in an inert atmosphere. The flow rate of the carrier gas was kept at 80 ml/min. To ensure the reliability of the experimental results, all experiments repeated three times to satisfy the reproducibility criteria and the relative error between the measured values was within 5%.

TABLE 2 Ultimate analysis, proximate analysis, and biochemical analysis of GBR sample.

Ultimate analysis	wt%	Proximate analysis	wt%	Biochemical analysis	wt%
Carbon	53.72	Volatiles	72.59	Cellulose	42.4
Hydrogen	7.74	Fixed carbon	14.65	Hemicelluloses	15.35
Oxygen	33.68	Ash	8.23	Lignin	29.37
Nitrogen	1.25	Moisture	4.53	Extractives	12.88
Sulfur	0.36				

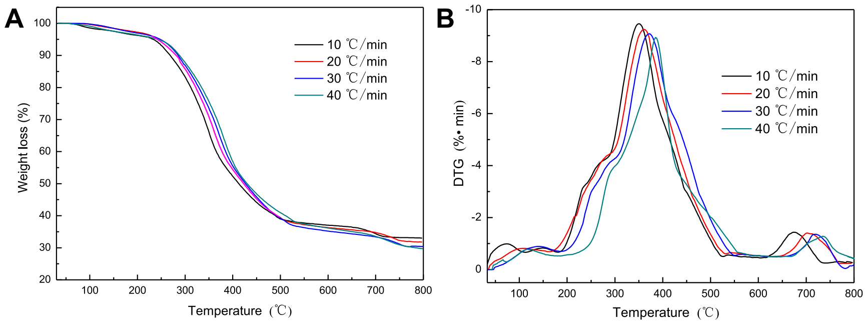

FIGURE 3
(A) TG curve of dregs at different heating rates, **(B)** DTG curve of dregs at different heating rates.

4.3 Effect of the heating rate on the thermogravimetric analysis

As shown in Figure 3, when the heating rate of pyrolysis process changed, the trend of raw materials was nearly not changed, which indicated that the pyrolysis mechanism of raw materials was consistent under different heating rates. However, the heating rate affected the peak value, the position of the inflection point of the highest temperature and the maximum decomposition rate of the TGA curve. Samuelsson et al. drew a similar experimental conclusion when they studied the pyrolysis of Norway spruce (Samuelsson et al., 2015). When the heating rates were 10 C/min, 20 C/min, 30 C/min and 40 C/min, the peak temperatures of the dregs were 337 C, 352 C, 362 C, and 380°C, respectively, and the maximum point of mass loss rate shifted to high temperature. This could be due to the limitations of the heat mass transfer in the sample, which resulted in the difference between the reference and the sample temperature. In addition, the poor thermal conductivity of biomass material also led to the temperature gradient in the experiment, that is, the temperature inside the sample might be lower than that of its surface. Furthermore, the maximum mass loss rate of the DTG curve decreased. The same phenomenon was observed by other researchers (Fernandez et al., 2016; Chandrasekaran et al., 2017).

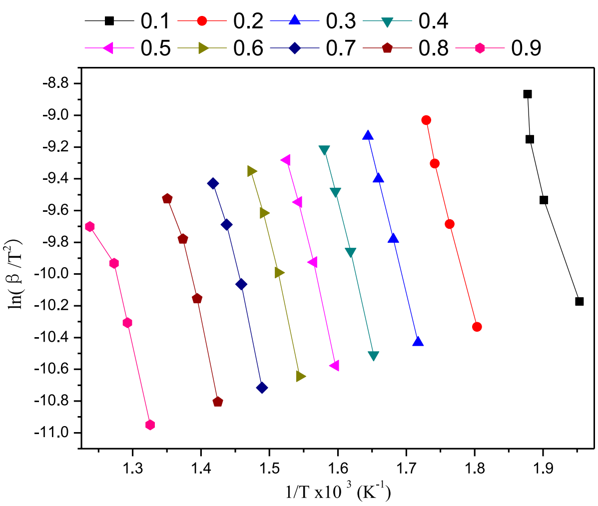

FIGURE 4
KAS method to find the fit curve of activation energy.

Therefore, when the temperature remained the same, heating rates was lower, the heat transfer between the biomass particles was higher. That resulted in the higher degree of pyrolysis and lower coke ash content. With higher heating rates, the thermal

TABLE 3 KAS method to obtain activation energy and correlation coefficient.

Conversion (α)	R^2	E (KJ/mol)
0.1	0.9210	130.36
0.2	0.9955	143.66
0.3	0.9999	147.56
0.4	0.9976	149.92
0.5	0.9940	151.35
0.6	0.9907	151.93
0.7	0.9835	150.76
0.8	0.9711	145.76
0.9	0.9071	119.1

hysteresis between the biomass particles resulted in partial non-devolatilization, which formed the coke with higher calorific value.

4.4 Pyrolysis kinetic analysis

4.4.1 Determination of activation energy

In this study, the KAS method was used to avoid selection of the mechanism function and directly obtain the activation energy E, thus reducing unnecessary errors during the calculation process. Figure 4 shows the fitting curve of the activation energy of a pesticide residue. When the conversion value was beyond the range of 0.2–0.8, the linear correlation coefficient of the obtained fitting curve was low (R2 < 0.95). Therefore, these fitting curves could not be used to estimate the activation energy of the pesticide residue. When the conversion value ranged from 0.2 to 0.8, the fitted curves had higher correlation coefficients (R2 > 0.97) and were basically parallel to each other, indicating that the apparent activation energy had small changes within this range and followed the same pyrolysis mechanism; thus, this range was suitable for the activation energy estimation.

Table 3 shows the activation energy E and correlation coefficient R2 obtained using the KAS method for dreg pyrolysis. As shown in Table 3, the activation energy increased and then decreased with the increase of the conversion value, which was basically consistent with the trend of castor pyrolysis reported by Kaur et al. (Kaur et al., 2018). When the conversion value ranged from 20 to 60%, hemicellulose and cellulose pyrolysis occurred, and the activation energy continued to rise. As the pyrolysis continued, the activation energy value decreased when the conversion value was between 60 and 80%. At this stage, lignin and cellulose with low residuals were pyrolyzed. Vamvuka et al. found that cellulose decomposition had the highest activation energy (145–285 kJ/mol), whereas lignin decomposition had the lowest activation energy (30–39 kJ/mol), which might be the reason for the reduced activation energy (Vamvuka et al., 2003). When the conversion value was between 20 and 80%, the average EKAS was 148.71 kJ/mol.

4.4.2 Determination of pyrolysis mechanism function

In this study, the Coats-Redfern method combined with 41 common solid-phase reaction mechanism functions was used to calculate the pyrolysis kinetic parameters E, A and the correlation coefficient R^2 at different heating rates *ß*. Partial results are listed in Table 4. If the selected pyrolysis kinetic function G(α) was reasonable, the activation energy E value obtained by the Coats-Redfern integral method should be similar to that obtained by the KAS method. Table 4 shows that the linear correlation coefficients R^2 of the equation fitted by the reactions and the Avrami-Erofeev model (n = 2, 3, 4) was high, but the E values obtained by these models were quite different. Only the mechanism function A-E using the reaction order $n = 3$ obtained an activation energy EA2 closest to EKAS (EA2 = 161.34 kJ/mol). Therefore, the pyrolysis stage of the GBR follows the A-E equation, and its reaction mechanism is random nucleation and growth. The reaction series n is equal to 3, and the mechanism function can be expressed as $G(\alpha) = [-\ln(1-\alpha)]^3$.

4.4.3 Kinetic compensation effect

As shown in Table 4, the heating rate is accordance with both ln*A* and E. This might be due to the type of interaction between In*A* and E, which is named the dynamic compensation effect. Besides, the E and In*A* of the dreg pyrolysis fitted linearly (as shown in Figure 5). The linear correlation coefficient R^2 of the fitted equation was 0.9811, and the dynamics compensation effect expression of the dregs was ln*A* = 0.2778E-16.3062. Thus, the frequency factor A of the dreg pyrolysis reaction was calculated and found to be approximately equal to 2.418 min × 1,012 min. The mechanism functions G(α), EKAS and A were substituted into Eq. 13 to get the kinetic equation for the dreg pyrolytic process as below:

$$\frac{d\alpha}{dT} = \left(\frac{2.418 \times 10^{12}}{\beta}\right) \exp\left(\frac{148.71 \times 10^{3}}{RT}\right) \cdot \frac{(1-\alpha)[-\ln(1-\alpha)]^{2}}{3} \tag{13}$$

4.5 GA-Adaboost evaluation

4.5.1 GA-Adaboost model setting

The main parameters that determines the performance of Adaboost model are the number of iterations and learning rate. Firstly, the value range of the two parameters was limited to 50–100 and 0.1-2 by empirical method and trial-and-error method. DNA length contained two parameters, each of which took up 12 bits. Each parameter had 212 valid values,

TABLE 4 Kinetic parameters of Coats-Redfern method for different heating rates.

Mechanism function	β = 10 C/min			β = 20 C/min		
	R^2	ln*A* (min^{-1})	*E* (kJ/mol)	R^2	ln*A* (min^{-1})	*E* (kJ/mol)
F1	0.9896	3.34	31.75	0.9841	4.07	32.74
F2	0.9894	7.50	48.50	0.9938	8.29	50.15
D1	0.9310	6.06	49.99	0.9182	6.78	51.34
D2	0.9572	6.98	56.46	0.9471	7.71	58.05
D3	0.9806	7.48	64.76	0.9739	8.25	66.66
A1	0.9936	11.84	73.74	0.9899	12.63	75.99
A2	0.9949	27.57	157.72	0.9919	28.21	160.49
A3	0.9945	19.94	115.73	0.9919	20.79	119.24
R1	0.9535	0.94	25.22	0.9413	1.66	25.96
R2	0.9690	1.08	27.25	0.9591	1.80	28.07
	β = 30°C/min			β = 40°C/min		
	R^2	lnA (min^{-1})	E (kJ/mol)	R^2	lnA (min^{-1})	E (kJ/mol)
F1	0.9853	4.36	32.69	0.9794	5.12	33.71
F2	0.9930	8.53	50.11	0.9933	9.14	51.45
D1	0.9207	7.04	51.38	0.9115	7.61	52.54
D2	0.9492	7.95	58.09	0.9418	8.46	59.98
D3	0.9754	8.46	66.70	0.9701	8.89	67.25
A1	0.9908	12.82	76.03	0.9872	13.16	76.21
A2	0.9926	28.81	162.72	0.9898	29.46	164.41
A3	0.9920	20.89	119.38	0.9890	21.80	120.71
R1	0.9435	1.96	25.91	0.9316	2.78	27.19
R2	0.9610	2.09	28.02	0.9514	2.90	29.23

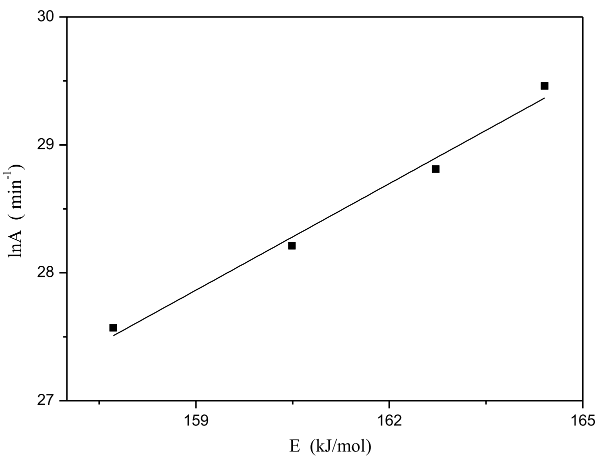

FIGURE 5
Kinetic compensation effect of dregs at different heating rates.

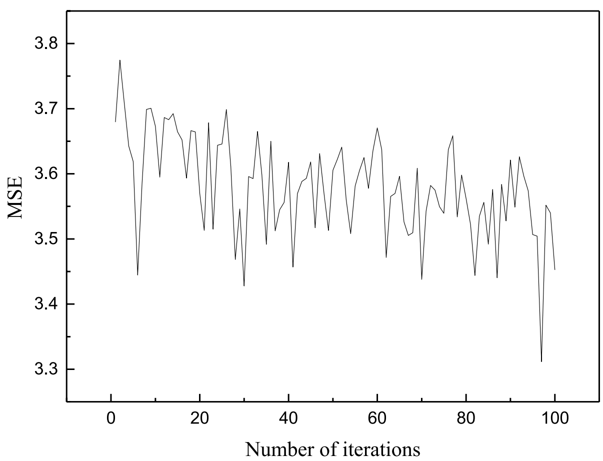

FIGURE 6
Variation curve iteration times and mean squared error.

10.3389/fenrg.2022.967856

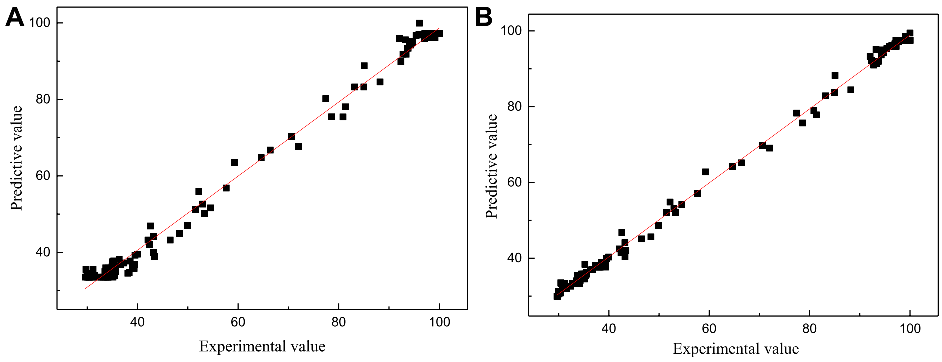

FIGURE 7
(A) Fitting diagram of Adaboost model on the test dataset, **(B)** Fitting diagram of GA-Adaboost model on the test dataset.

and the total DNA length was 24. The DNA population was set to 200. The mating probability of paternal population was 50%. The mutation probability of each DNA was 0.1%. The number of iterations was 100.

4.5.2 Comparison of adaboost and GA-Adaboost models

When the genetic algorithm was used to adjust the parameters, all valid samples with the amount of 1,303 would be used to obtain results of parameters selection. During the verification process, in order to obtain an intuitive comparison, the data were randomly sampled, 80% of the data were used for training, and remaining 20% data were used for validation. Adaboost model and GA-Adaboost model with default parameters (the rounds of iterations is 50 and the learning rate is 0.1) were used to train the data. The performance of the model had been verified by the validation data after the two models were established. This study used mean squared error (MSE) as the algorithm loss function for performance verification.

The number of iterations was determined by observing the error change of the test samples during iteration. Using Adaboost algorithm, the number of iterations usually was within (1, 100). Each iteration ran five times. The average value of the five running errors was taken as the evaluation index of the final strong predictor error, as shown in Figure 6. The number of iterations corresponding to the minimum average test error was chosen as the iteration constant of GA-Adaboost model to avoid over learning. It can be seen from the figure that due to the existence of mutation; the loss function was gradually fluctuating falling, which shows that the mutation mechanism can effectively help the algorithm jump out of the local optimum and realize further iteration. Therefore, in this study, the number of iterations was 88 and the learning rate was 1.5485.

The Adaboost model had fitting degree of 99.38% on training data, 99.26% on verification data, and MSE was 4.9653. The GA-Adaboost model had a fitting degree of 99.88% on training data, 99.80% on verification data, and MSE was 3.4173. Figure 6 is the fitting diagram of test data. It can be found that the fitting degree of the two models is very high, so the difference between the two models cannot be seen directly. However, the MSE of Adaboost model was 4.9653, while GA-Adaboost can reduce the mean squared error by 31.18%. This proves that the performance of Adaboost model adjusted by GA algorithm has significant advantages. As shown in Figure 7, we can see that the GA-Adaboost runs are closer to the 45° fit line. On the other hand, the fit of GA-Adaboost on the validation dataset is close to the fit of the Adaboost model with default parameters on the training dataset. Therefore, compared with Adaboost model with default settings, GA-Adaboost model achieved better performance while predicting the pyrolysis process of ginkgo biloba residue.

5 Conclusion

In this study, in order to improve the reaction efficiency of GBR Pyrolysis, the thermodynamic and parameters of GBR were systematically studied, and a GA and Adaboost algorithm based method was proposed to predict the combustion trend. The thermal analysis of TG and DTG showed that the pyrolysis of GBR includes a number of complex reaction mechanism. A Coats-Redfern model based analysis of the thermal kinetics of GBR indicated that the optimal reaction mechanism was random nucleation. The pyrolysis kinetic model at different heating rates was established in the experiment. The introduced GA-Adaboost model achieved good performance (with a fitting degree of 99.88% on training data, 99.80% on verification data, and MSE of 3.4173) while predicting the pyrolysis process of GBR. Various kinetic parameters and TG data in pyrolysis can be observed through these predicted data by GA-Adaboost model. These parameters were proved (by the experiment) valid for the pyrolysis process of GBR.

Data availability statement

The raw data supporting the conclusions of this article will be made available by the authors, without undue reservation.

Author contributions

LL and JC proposed the research plan. LL, JC, ZY, ZC, KW, and QX completed the experiment and manuscript draft. JC revised the primitive draft of the manuscript and completed the formal manuscript for submission.

Funding

This work is supported by the 2022 introducing Talents Start-up Project in Zhejiang shuren university (KXJ0622605),the 2020 Basic Scientific Research Project of Provincial Universities in Zhejiang (2021XZ009) and the 2020 Basic Scientific Research Project of Zhejiang Tongji Vocational College of Science and Technology (FRF20PY001).

Conflict of interest

The authors declare that the research was conducted in the absence of any commercial or financial relationships that could be construed as a potential conflict of interest.

Publisher's note

All claims expressed in this article are solely those of the authors and do not necessarily represent those of their affiliated organizations, or those of the publisher, the editors and the reviewers. Any product that may be evaluated in this article, or claim that may be made by its manufacturer, is not guaranteed or endorsed by the publisher.

References

Bai, X., Wang, G., Sun, Y., Yu, Y., Liu, J., Wang, D., et al. (2018). Effects of combined pretreatment with rod-milled and torrefaction on physicochemical and fuel characteristics of wheat straw. *Bioresour. Technol.* 267, 38–45. doi:10.1016/j.biortech.2018.07.022

Barbado, R., Araque, O., and Iglesias, C. A. (2019). A framework for fake review detection in online consumer electronics retailers. *Inf. Process. Manag.* 56 (4), 1234–1244. doi:10.1016/j.ipm.2019.03.002

Chandrasekaran, A., Ramachandran, S., and Subbiah, S. (2017). Determination of kinetic parameters in the pyrolysis operation and thermal behavior of Prosopis juliflora using thermogravimetric analysis. *Bioresour. Technol.* 233, 413–422. doi:10.1016/j.biortech.2017.02.119

Chen, J., Li, C., Ristovski, Z., Milic, A., Gu, Y., Islam, M. S., et al. (2017). A review of biomass burning: Emissions and impacts on air quality, health and climate in China. *Sci. Total Environ.* 579, 1000–1034. doi:10.1016/j.scitotenv.2016.11.025

Chen, L., Wang, S., Meng, H., Wu, Z., and Zhao, J. (2017). Synergistic effect on thermal behavior and char morphology analysis during co-pyrolysis of paulownia wood blended with different plastics waste. *Appl. Therm. Eng.* 111, 834–846. doi:10.1016/j.applthermaleng.2016.09.155

Collazzo, G. C., Broetto, C. C., Perondi, D., Junges, J., Dettmer, A., Dornelles Filho, A., et al. (2017). A detailed non-isothermal kinetic study of elephant grass pyrolysis from different models. *Appl. Therm. Eng.* 110, 1200–1211. doi:10.1016/j.applthermaleng.2016.09.012

De Sales, C. A. V. B., Maya, D. M. Y., Lora, E. E. S., Jaen, R. L., Reyes, A. M. M., Gonzalez, A. M., et al. (2017). Experimental study on biomass (eucalyptus spp.) gasification in a two-stage downdraft reactor by using mixtures of air, saturated steam and oxygen as gasifying agents. *Energy Convers. Manag.* 145, 314–323. doi:10.1016/j.enconman.2017.04.101

EsmaeiliKelishomi, A., Garmabaki, A. H. S., Bahaghighat, M., and Dong, J. (2019). Mobile user indoor-outdoor detection through physical daily activities. *Sensors* 19 (3), 511. doi:10.3390/s19030511

Fernandez, A., Saffe, A., Pereyra, R., Mazza, G., and Rodriguez, R. (2016). Kinetic study of regional agro-industrial wastes pyrolysis using non-isothermal TGA analysis. *Appl. Therm. Eng.* 106, 1157–1164. doi:10.1016/j.applthermaleng.2016.06.084

Ferreira, A. D., Freitas, D. M., da Silva, G. G., Pistori, H., and Folhes, M. T. (2017). Weed detection in soybean crops using ConvNets. *Comput. Electron. Agric.* 143, 314–324. doi:10.1016/j.compag.2017.10.027

Ferreira, J. M., Pires, I. M., Marques, G., Garcia, N. M., Zdravevski, E., Lameski, P., et al. (2020). Identification of daily activites and environments based on the adaboost method using mobile device data: A systematic review. *Electronics* 9 (1), 192. doi:10.3390/electronics9010192

Fitzpatrick, E., Bachenko, J., and &Fornaciari, T. (2015). Automatic detection of verbal deception. *Synthesis Lect. Hum. Lang. Technol.* 8 (3), 1–119. doi:10.2200/s00656ed1v01y201507hlt029

Freund, Y., and Schapire, R. E. (1996). Experiments with a new boosting algorithm[C]. *icml* 96, 148–156.

Freund, Y. (1995). Boosting a weak learning algorithm by majority. *Inf. Comput.* 121 (2), 256–285. doi:10.1006/inco.1995.1136

Gai, K., Qiu, M., and Zhao, H. (2017). Cost-aware multimedia data allocation for heterogeneous memory using genetic algorithm in cloud computing. *IEEE Trans. Cloud Comput.* 8 (99), 1212–1222. doi:10.1109/tcc.2016.2594172

Guerrero, C., Isaac, L., and Juiz, C. (2018). Genetic algorithm for multi-objective optimization of container allocation in cloud architecture. *J. Grid Comput.* 161, 113–135. doi:10.1007/s10723-017-9419-x

Guo, F., Dong, Y., Dong, L., and Jing, Y. (2013). An innovative example of herb residues recycling by gasification in a fluidized bed. *Waste Manag.* 33 (4), 825–832. doi:10.1016/j.wasman.2012.12.009

Holland, J. H. (1992). *Adaptation in natural and artificial systems: An introductory analysis with applications to biology, control, and artificial intelligence*. MIT press.

Huang, L., Yin, Y., Fu, Z., Zhang, S., Deng, H., and Liu, D. (2020). LoAdaBoost: Loss-based AdaBoost federated machine learning with reduced computational complexity on IID and non-IID intensive care data. *Plos one* 15 (4), e0230706. doi:10.1371/journal.pone.0230706

Kaur, R., Gera, P., Jha, M. K., and Bhaskar, T. (2018). Pyrolysis kinetics and thermodynamic parameters of castor (Ricinus communis) residue using thermogravimetric analysis. *Bioresour. Technol.* 250, 422–428. doi:10.1016/j.biortech.2017.11.077

Li, H., Xu, B., Lu, G., Du, C., and Huang, N. (2021). Multi-objective optimization of PEM fuel cell by coupled significant variables recognition, surrogate models and a multi-objective genetic algorithm. *Energy Convers. Manag.* 236, 114063. doi:10.1016/j.enconman.2021.114063

Li, K. J., Sha, Z. D., Chen, W. P., Xue, X., Mao, H. P., and Tan, G. (2020). A fast modeling and optimization scheme for greenhouse environmental system using proper orthogonal decomposition and multi-objective genetic algorithm. *Comput. Electron. Agric.* 168, 105096. doi:10.1016/j.compag.2019.105096

Liang, W., Hu, Y., Zhou, X., Pan, Y., and Wang, K. (2021). Variational few-shot learning for microservice-oriented intrusion detection in distributed industrial IoT. *IEEE Trans. Ind. Inf.* 18, 5087–5095. doi:10.1109/TII.2021.3116085

Lu, F., Zhang, Z., Guo, L., Chen, J., Zhu, Y., Yan, K., et al. (2022). HFENet: A lightweight hand-crafted feature enhanced CNN for ceramic tile surface defect detection. *Int. J. Intell. Syst.* doi:10.1002/int.22935

Mayer, M. J., Szilágyi, A., and Gróf, G. (2020). Environmental and economic multi-objective optimization of a household level hybrid renewable energy system by genetic algorithm. *Appl. Energy* 269, 115058. doi:10.1016/j.apenergy.2020.115058

Mehmood, M. A., Ye, G., Luo, H., Liu, C., Malik, S., Afzal, I., et al. (2017). Pyrolysis and kinetic analyses of Camel grass (Cymbopogon schoenanthus) for bioenergy. *Bioresour. Technol.* 228, 18–24. doi:10.1016/j.biortech.2016.12.096

Minh Loy, A. C., Yusup, S., Fui Chin, B. L., Wai Gan, D. K., Shahbaz, M., Acda, M. N., et al. (2018). Comparative study of *in-situ* catalytic pyrolysis of rice husk for syngas production: Kinetics modelling and product gas analysis. *J. Clean. Prod.* 197, 1231–1243. doi:10.1016/j.jclepro.2018.06.245

Mishra, R. K., and Mohanty, K. (2018). Pyrolysis kinetics and thermal behavior of waste sawdust biomass using thermogravimetric analysis. *Bioresour. Technol.* 251, 63–74. doi:10.1016/j.biortech.2017.12.029

Nazoktabar, M., Jazayeri, S. A., Arshtabar, K., and Ganji, D. D. (2018). Developing a multi-zone model for a HCCI engine to obtain optimal conditions using genetic algorithm. *Energy Convers. Manag.* 157, 49–58. doi:10.1016/j.enconman.2017.12.001

Oluoti, K., Doddapaneni, T. R. K. C., and Richards, T. (2018). Investigating the kinetics and biofuel properties of Alstoniacongensis and Ceiba pentandra via torrefaction. *Energy* 150, 134–141. doi:10.1016/j.energy.2018.02.086

Panapakidis, I. P., and Dagoumas, A. S. (2017). Day-ahead natural gas demand forecasting based on the combination of wavelet transform and ANFIS/genetic algorithm/neural network model. *Energy* 118, 231–245. doi:10.1016/j.energy.2016.12.033

Paykani, A., Frouzakis, C. E., and Boulouchos, K. (2019). Numerical optimization of methane-based fuel blends under engine-relevant conditions using a multi-objective genetic algorithm. *Appl. Energy* 242, 1712–1724. doi:10.1016/j.apenergy.2019.03.041

Pelaez-Samaniego, M. R., Yadama, V., Lowell, E., and Espinoza-Herrera, R. (2013). Erratum to: A review of wood thermal pretreatments to improve wood composite properties. *Wood Sci. Technol.* 47 (6), 1321–1322. doi:10.1007/s00226-013-0577-0

Qiu, M., Ming, Z., Li, J., Gai, K., and Zong, Z. (2015). Phase-change memory optimization for green cloud with genetic algorithm. *IEEE Trans. Comput.* 64 (12), 3528–3540. doi:10.1109/TC.2015.2409857

Samuelsson, L. N., Babler, M. U., and Moriana, R. (2015). A single model-free rate expression describing both non-isothermal and isothermalpyrolysisofNorway Spruce. *Fuel* 161, 59–67. doi:10.1016/j.fuel.2015.08.019

Shen, G., Zhu, D., Chen, J., and Kong, X. (2022). Motif discovery based traffic pattern mining in attributed road networks. *Knowl. Based. Syst.* 250, 109035. doi:10.1016/j.knosys.2022.109035

Singh, V., Vaibhav, S., and Singh, V. (2020). Fuel consumption optimisation using structural equation modelling and genetic algorithm approach: The case of commercial aviation. *Eur. Transport/Trasporti Eur.* 78 (2), 1–21. doi:10.48295/et.2020.78.2

Starke, A. R., Cardemil, J. M., Escobar, R., and Colle, S. (2018). Multi-objective optimization of hybrid CSP+PV system using genetic algorithm. *Energy* 147, 490–503. doi:10.1016/j.energy.2017.12.116

Vamvuka, D., Kakaras, E., Kastanaki, E., and Grammelis, P. (2003). Pyrolysis characteristics and kinetics of biomass residuals mixtures with lignite. *Fuel* 82 (15-17), 1949–1960. doi:10.1016/s0016-2361(03)00153-4

Wang, L., Wang, P., Liang, S., Zhu, Y., Khan, J., and Fang, S. (2020). Monitoring maize growth on the North China Plain using a hybrid genetic algorithm-based back-propagation neural network model. *Comput. Electron. Agric.* 170, 105238. doi:10.1016/j.compag.2020.105238

Wang, W., and Sun, D. (2021). The improved AdaBoost algorithms for imbalanced data classification. *Inf. Sci.* 563, 358–374. doi:10.1016/j.ins.2021.03.042

Yan, K., Chen, X., Zhou, X., Yan, Z., and Ma, J. (2022). Physical model informed fault detection and diagnosis of air handling units based on transformer generative adversarial network. *IEEE Trans. Ind. Inf.*, 1–8. doi:10.1109/TII.2022.3193733

Yan, K. (2021). Chiller fault detection and diagnosis with anomaly detective generative adversarial network. *Build. Environ.* 201, 107982. doi:10.1016/j.buildenv.2021.107982

Yan, K., Zhou, X., and Chen, J. (2022). Collaborative deep learning framework on IoT data with bidirectional NLSTM neural networks for energy consumption forecasting. *J. Parallel Distributed Comput.* 163, 248–255. doi:10.1016/j.jpdc.2022.01.012

Yu, Z. W., Gao, Q., Zhang, Y., Wang, D. D., Nyalala, I., and Chen, K. J. (2019). Production of activated carbon from sludge and herb residue of traditional Chinese medicine industry and its application for methylene blue removal. *Bioresources* 14 (1), 1333–1346. doi:10.15376/biores.14.1.1333-1346

Yu, Z., Yousaf, K., Ahmad, M., Yousaf, M., Gao, Q., and Chen, K. (2020). Efficient pyrolysis of ginkgo biloba leaf residue and pharmaceutical sludge (mixture) with high production of clean energy: Process optimization by particle swarm optimization and gradient boosting decision tree algorithm. *Bioresour. Technol.* 304, 123020. doi:10.1016/j.biortech.2020.123020

Zhan, X., and Yu, S. (2020). Reconstructing the historical patterns of forest stand based on CA-AdaBoost-ANN model. *For. Ecol. Manag.* 478, 118518. doi:10.1016/j.foreco.2020.118518

Zhang, S. A., Chen, Y., Zhang, W. Y., and Feng, R. J. (2021). A novel ensemble deep learning model with dynamic error correction and multi-objective ensemble pruning for time series forecasting. *Inf. Sci.* 544, 427–445. doi:10.1016/j.ins.2020.08.053

Zhang, S., Su, Y., Xu, D., Zhu, S., Zhang, H., and Liu, X. (2018). Assessment of hydrothermal carbonization and coupling washing with torrefaction of bamboo sawdust for biofuels production. *Bioresour. Technol.* 258, 111–118. doi:10.1016/j.biortech.2018.02.127

Zhou, X., Hu, Y., Wu, J., Liang, W., Ma, J., and Jin, Q. (2022). Distribution bias aware collaborative generative adversarial network for imbalanced deep learning in industrial IoT. *IEEE Trans. Ind. Inf.*, 1. doi:10.1109/TII.2022.3170149

Zhou, X., Liang, W., Li, W., Yan, K., Shimizu, S., and Wang, K. (2021). Hierarchical adversarial attacks against graph neural network based IoT network intrusion detection system. *IEEE Internet Things J.* 9, 9310–9319. doi:10.1109/JIOT.2021.3130434

Zhou, X., Liang, W., Shimizu, S., Ma, J., and Jin, Q. (2021). Siamese neural network based few-shot learning for anomaly detection in industrial cyber-physical systems. *IEEE Trans. Ind. Inf.* 17 (8), 5790–5798. doi:10.1109/TII.2020.3047675

Zhou, X., Liang, W., Yan, K., Li, W., Wang, K., Ma, J., et al. (2022). Edge enabled two-stage scheduling based on deep reinforcement learning for internet of everything. *IEEE Internet Things J.* doi:10.1109/JIOT.2022.3179231

Zhou, X., Yang, X., Ma, J., and Wang, K. (2021). Energy efficient smart routing based on link correlation mining for wireless edge computing in IoT. *IEEE Internet Things J.* doi:10.1109/JIOT.2021.3077937